

Fluctuation effects in the microwave conductivity of cuprate superconductors

J. R. Waldram, D. M. Broun, D. C. Morgan, and R. Ormeno
Cavendish Laboratory and IRC in Superconductivity, Cambridge CB3 0HE, United Kingdom

A. Porch

School of Electronic and Electrical Engineering, University of Birmingham, Birmingham B15 2TT, United Kingdom
 (Received 27 October 1997)

Observations on the surface impedance at 14, 25, and 36 GHz of high quality crystals of $\text{Bi}_2\text{Sr}_2\text{CaCu}_2\text{O}_{8+x}$ (Bi2212), $\text{Tl}_2\text{Ba}_2\text{CuO}_6$ (Tl2201), and $\text{YBa}_2(\text{Cu}_{0.975}\text{Zn}_{0.025})_3\text{O}_{7-\delta}$ (Y123/Zn) are reported, and the corresponding complex conductivity $\sigma = \sigma' - i\sigma''$ is analyzed in the critical region near T_c and at higher temperatures where fluctuations are important. The well known sharp peak in σ' within the critical region is successfully analyzed using effective medium theory. At higher temperatures Bi2212 and Y123/Zn agree in form with the treatment of conductivity fluctuations of Aslamazov and Larkin, extended to high frequency. Tl2201, however, shows an extra response of long relaxation time which persists at high temperatures. Tentative explanations of this effect are considered, including the possibility that it is due to uncondensed bipolarons. The physics of conversion of supercurrent to normal current within fluctuating regions is reviewed. [S0163-1829(99)10401-6]

I. INTRODUCTION

We have recently measured the surface impedance $Z_s = (i\omega\mu_0/\sigma)^{1/2}$ for current flow in the a - b plane of high quality single crystals of $\text{Bi}_2\text{Sr}_2\text{CaCu}_2\text{O}_{8+x}$ (Bi2212), $\text{Tl}_2\text{Ba}_2\text{CuO}_6$ (Tl2201), and $\text{YBa}_2(\text{Cu}_{0.975}\text{Zn}_{0.025})_3\text{O}_{7-\delta}$ (Y123/Zn) at several microwave frequencies.¹ Typical results are shown in Fig. 1. The corresponding real and imaginary parts of the microwave conductivity $\sigma = \sigma' - i\sigma''$ are shown in Fig. 2. As we shall report elsewhere, at temperatures below T_c these conductivities have been successfully fitted to the two-fluid model of cuprate conductivity,² in the sense that we can fit the data at all three frequencies with a normal fraction $f_n(T)$ which fits the d -wave model of cuprate superconductivity, and a normal current relaxation time $\tau(T)$, which is linear in T at low temperatures, contrary to

current theories. In this paper we shall be concerned with the microwave conductivity in regions where fluctuations are important, and our aim is to address the question of whether the microwave observations may be explained in terms of fluctuation effects alone.

The reliability of our experimental methods is discussed in Secs. II and IV. In Sec. III we discuss the microwave conductivity in the normal state above T_c , where the fluctuations are relatively small. Fluctuations in this temperature range are known to increase the heat capacity and to reduce the dc resistivity ρ_{dc} , and these effects have been successfully analyzed using Ginzburg-Landau theory and other methods.³ We shall show that for Bi2212 and Y123/Zn our results agree well with this theory (if some scaling is permitted for the Y123/Zn sample). However, as Fig. 2 shows, in Tl2201 we found a relatively large imaginary conductivity

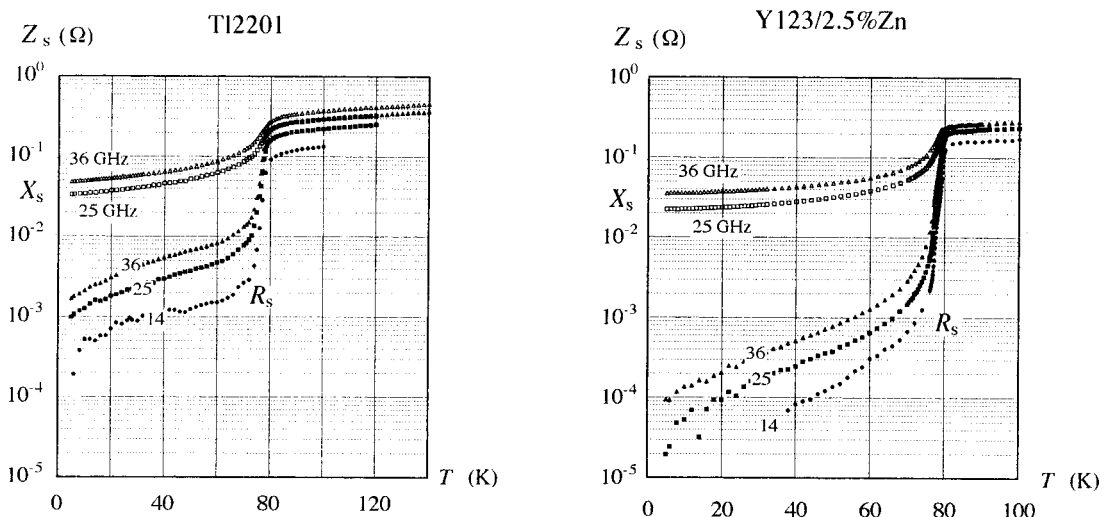


FIG. 1. Real and imaginary parts of the surface impedance of two samples for current flow in the a - b plane, labeled with frequency in GHz. X_s could not be measured accurately at 14 GHz.

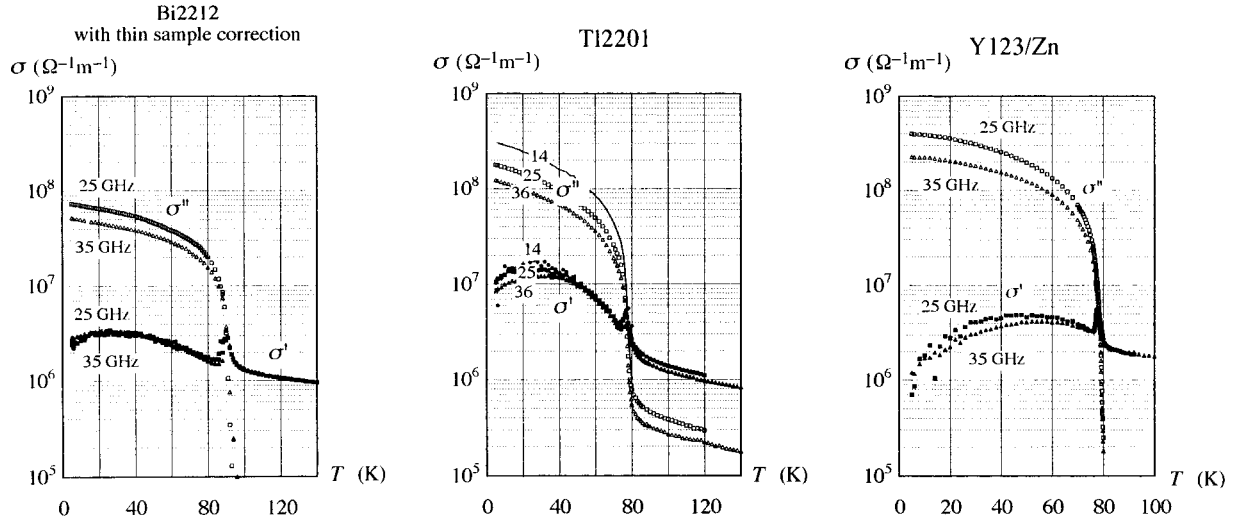


FIG. 2. Conductivities in ab plane deduced from surface impedance. The $\sigma'(T)$ values shown for Tl2201 at 14 GHz were deduced assuming that $\sigma''(T) \propto 1/\omega$ below 73 K (solid line).

σ'' above T_c , which could not be explained by the standard theory of small fluctuations. We discuss this phenomenon in Secs. V and VI.

In the immediate neighborhood of T_c there is a sharp peak in σ' , which has been observed in many cuprates.⁴ It becomes higher as the frequency falls and was originally interpreted as a narrowed BCS coherence peak, but is now more often ascribed to the effect of critical fluctuations. We shall discuss the conductivity in this range of temperature in Sec. VII.

II. EXPERIMENTAL DETAILS

The samples all took the form of plates thin in the c -direction. The Bi2212 samples used were cut from crystals prepared at NRIM STA, Tsukuba by Mochiku using the traveling solvent floating zone method, and were typically about 1 mm \times 1 mm in the ab plane \times 6 μ m in the c direction. Further details of preparation of the Bi2212 sample are given in Ref. 5. The sole Tl2201 sample was a slightly overdoped single crystal of $\text{Tl}_{1.85}\text{Ba}_2\text{Cu}_{1.15}\text{O}_{6+\delta}$ made in our laboratory by Mackenzie and Tyler. This was grown by a self-flux method in an alumina crucible and annealed in flowing 5% H_2/Ar gas at 420 $^\circ\text{C}$ for 10 days. The crystal had dimensions 0.15 mm \times 0.3 mm in the ab plane \times 10 μ m in the c direction and was chosen for the narrowness of its rf transition. The Y123/Zn crystal was grown from flux in Y_2O_3 crucibles by Cheng and Hodby at the University of Oxford and annealed in flowing O_2 gas at 420 $^\circ\text{C}$ for 15 days. Electron microprobe analysis and the value of T_c give consistent values for the concentration of Zn.

The resonator perturbation techniques used to measure surface impedance are described in detail elsewhere.⁶ The sample, supported on a sapphire rod, is introduced into the resonator through a small hole in the wall. At 25 and 36 GHz, the resonators are cylindrical superconducting TE_{011} cavities, while at 14 GHz a TE_{011} sapphire dielectric resonator in a superconducting enclosure is used. In all cases, the resonators are maintained at 4.2 K while the sample is heated

independently via the sapphire rod. In this way, high Q factors, of the order of 10^6 – 10^7 , are achieved and systematic error is kept to a minimum.

In each case the sample is placed accurately normal to the rf B field on the cylindrical axis of the resonator; the microwave currents flow in the ab plane, and it is the corresponding surface impedance which is measured. Changes in the surface resistance R_s and the surface reactance X_s are proportional to the corresponding measured changes in the half-bandwidth and frequency of resonance, and the system is calibrated using a chemically polished Nb replica of the sample, whose surface impedance may be computed from its measured dc conductivity, for $T > 50$ K where the anomalous skin effect is insignificant. To fix the origin from which R_s is measured we assume that the change in bandwidth on adding the sample is due solely to its surface resistance. (Independent checks on losses in the vacuum grease and the effects of dummy samples in screening the sapphire rod confirm the validity of this assumption.) We cannot make a similar assumption for X_s because adding the sample excludes rf magnetic flux from a volume larger than the sample volume, of order L^3 where L is a typical ab dimension of the plate, and this causes a large frequency shift. (Indeed, it is important to check that this large frequency shift does occur: for some samples it was too small, suggesting that the rf flux is penetrating the sample along cracks or weak links.) However, at low temperatures we have $X_s = \omega \mu_0 \lambda_0$, so we fixed the origin from which changes in X_s are measured by using values of λ_0 of 2.1×10^{-7} m for Bi2212, measured by SQUID magnetometer, and of 1.7×10^{-7} m for Tl2201, from μ SR measurements.⁷ For Y123/Zn we had no precise value for λ_0 , so we assumed instead that $X_s = R_s$ at the highest temperature available; this is based on the assumption that σ is real and independent of frequency at this temperature, the usual assumption in the normal state, and it leads to a value of λ_0 of approximately 1.2×10^{-7} m.

In our samples of Bi2212 the normal state microwave skin depth was about one third of the sample thickness, large enough to make the thin sample correction important. In ex-

tracting the conductivity we assumed that the measured surface impedance Z_m was given by the standard expression for a sample of thickness $2a$ carrying a current symmetrical about the midplane

$$Z_m = Z_s \coth \frac{a}{\delta}, \quad (1)$$

where Z_s is the usual bulk surface impedance and δ is the complex skin depth $Z_s/i\omega\mu_0$. This expression is not accurate for the small part of the current flowing on the edge of the sample, so our results for Bi2212 must be treated with caution; but the correction is not very large and becomes negligible in the superconducting state.

III. THE THEORY OF ASLAMAZOV AND LARKIN

A detailed theory of the electrical conductivity in the region of small fluctuations above T_c was published in 1968 by Aslamazov and Larkin.⁸ For three- and two-dimensional superconductors they predicted that the fluctuating order parameter leads to extra components in the dc conductivity of the forms

$$\sigma_{\text{fluc3D}} = \frac{e^2}{32\hbar\xi_0} \left(\frac{T}{T-T_c} \right)^{1/2}, \quad \sigma_{\text{fluc2D}} = \frac{e^2}{16\hbar t} \frac{T}{T-T_c}, \quad (2)$$

where ξ_0 is the BCS coherence length and t is the thickness of the two dimensional structure; these components are to be added to the usual conductivity due to single particle excitations. Their method used superconductive perturbation theory at a fundamental level.

The forms of these predictions may be understood by using the Ginzburg-Landau theory of small fluctuations.³ The free energy stored in a fluctuating volume V will be of order $\alpha n_s V$, where α is the usual Ginzburg-Landau parameter and n_s is the nonequilibrium number density of superelectrons. This free energy will be of order kT . If the fluctuations are on a scale ξ_{GL} we deduce that $n_s \approx kT/\alpha\xi_{\text{GL}}^3$ for three-dimensional fluctuations and $n_s \approx kT/\alpha\xi_{\text{GL}}^2 t$ for two-dimensional fluctuations. In a two-dimensional system, the fraction of condensed electrons corresponding to n_s is of order $kT/2\pi\epsilon_F$, about 1% in a typical cuprate; this implies that $\Delta \approx 0.2kT$. If we assume that the fluctuating superelectrons respond to an electric field by accelerating in the usual way, but that the supercurrent decays with the Ginzburg-Landau relaxation time $\tau_{\text{GL}} = \pi\hbar/8k(T-T_c)$, we obtain extra contributions to the dc conductivity of order $n_s e^2 \tau_{\text{GL}}/m^*$, which may be rewritten as $\sigma_{\text{fluc3D}} \approx (e^2/\hbar\xi_0)(T/T_c - 1)^{-1/2}$ and $\sigma_{\text{fluc2D}} \approx (e^2/\hbar t)(T/T_c - 1)^{-1}$, the forms of Eq. (2).

A measure of the dc fluctuation conductivity may be obtained by subtracting from the observed conductivity a normal excitation contribution $\sigma_0(T)$ obtained by extrapolation from higher temperatures [usually assuming that $1/\sigma_0(T) \propto T$], and the Aslamazov and Larkin expressions have been successfully fitted to observations in this way for various cuprate superconductors.⁹ In Fig. 3(a) we show the temperature plot of inverse dc fluctuation conductivity for a Tl2201 crystal from the same batch as our microwave sample.⁵ This sample was slightly inhomogeneous, which has the effect of broadening the critical region, but it shows behavior of the

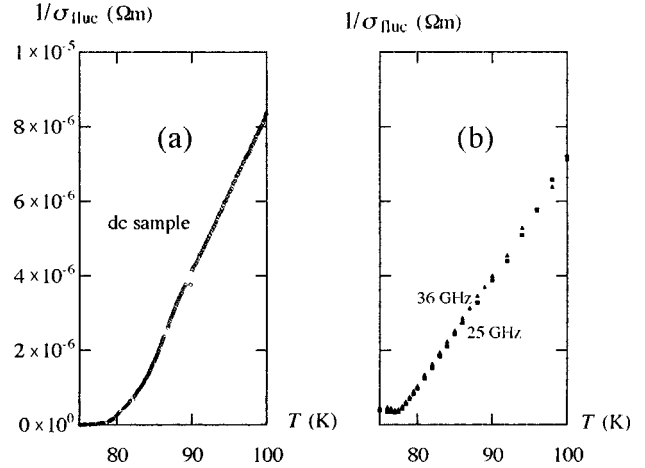


FIG. 3. (a) Inverse fluctuation conductivity of a sample of Tl2201, deduced from its dc conductivity. (b) Equivalent plots obtained in the same way from $\sigma'(T)$ at 25 and 36 GHz.

two-dimensional form above 87 K. However, the observed magnitude of σ_{fluc} is about half the predicted magnitude, if we assume that the appropriate value for t in Tl2201 is the spacing between the CuO_2 layers.

It seemed natural to us to extend the Aslamazov and Larkin theory to high frequencies by writing

$$\sigma = \sigma_0(T) + \frac{\sigma_{\text{fluc2D}}(T)}{1 + i\omega\tau_{\text{GL}}}, \quad (3)$$

where σ_0 is the normal dc conductivity due to excitations and $\sigma_{\text{fluc2D}}(T)$ is the dc fluctuation conductivity predicted by Aslamazov and Larkin. Equation (3) assumes that the supercurrent responds in the usual way for a carrier whose current decays with relaxation time τ_{GL} and that the normal excitation current has a relaxation time much shorter than $1/\omega$. The predicted values of $\omega\tau_{\text{GL}}$ are quite small at the frequencies and temperatures of interest, and Eq. (3) then predicts that $\sigma' \approx \sigma_{\text{dc}}$. We should therefore be able to fit the Aslamazov and Larkin theory to σ' in the usual way, defining σ_{fluc} as $\sigma' - \sigma_0$. The result for Tl2201 is shown in Fig. 3(b). We again find good agreement in form with the two-dimensional theory at both frequencies (and the magnitude in reasonable agreement with our dc result). Moreover, the critical region extends only up to about 78 K, about 2 K above T_c . This corresponds to the width of the critical region seen in dc conductivity or heat capacity in the best samples, suggesting that our sample is considerably more homogeneous than the dc sample considered earlier. Essentially similar results were found for the Bi2212 and Y123/Zn samples, both showing two-dimensional behavior.

Equation (3) also predicts σ'' , and we show in Fig. 4 a comparison of our data for σ_{fluc} and σ'' in Y123/Zn with the theoretical predictions (we have taken t to be the cell parameter c , assuming that the two adjacent CuO_2 planes fluctuate as a unit). When $\omega_{\text{GL}}\tau$ is small we expect $\sigma_{\text{fluc}} \propto (T-T_c)^{-1}$ and $\sigma'' \propto (T-T_c)^{-2}$, with slopes of -1 and -2 in this plot. Evidently our data have roughly the predicted form, and could be brought into approximate coincidence with the theory if we double t and simultaneously scale down τ_{GL} by about 30%. (Our fits are to the 2D theory, which does not

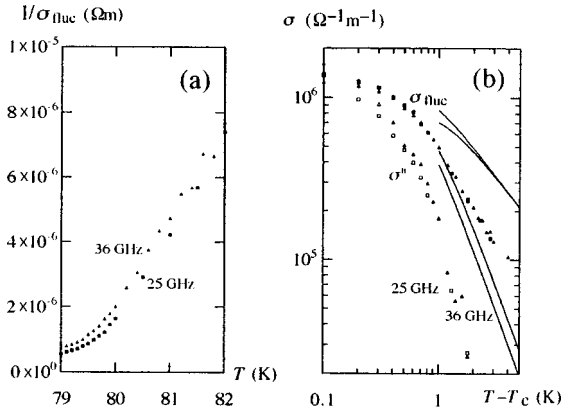


FIG. 4. Test of Aslamazov and Larkin theory for Y123/Zn. (a) Inverse fluctuation conductivity as a function of T ; two-dimensional behavior is apparent above 80 K. (b) Log-log plot of σ_{fluc} and σ'' against $T - T_c$. The solid lines show the theoretical predictions, with t taken to be c .

involve ξ_0 , but we remark that our Y123/Zn sample contains so little Zn that it remains near the clean limit, and the effective value of ξ_0 should remain close to the value for Y123. We therefore do not expect abnormally large fluctuations in this sample.) In a similar fit for Bi2212, on the other hand, we find the best agreement without scaling, if we take $t = c$. For Tl2201, although our results for $\sigma'(T)$ above the critical region are similar to those for Bi2212 and Y123/Zn, our results for $\sigma''(T)$ are very different, and cannot be fitted by Aslamazov and Larkin theory.

IV. CRITIQUE OF EXPERIMENTAL DATA ON Tl2201

At 20 K or more above T_c the fluctuation conductivity should be negligible, and we therefore expect the conductivity at microwave frequencies to be real and independent of frequency, with $R_s \propto \omega^{1/2}$ and $X_s = R_s$; and this is what we find in samples of Bi2212 and Y123. However, examination of Fig. 1(a) shows that neither of these expectations was true for our observations on Tl2201. We have not so far been able to obtain another sample of the quality needed for this work, and have therefore spent some effort in reviewing possible experimental errors which might explain these discrepancies.

The most obvious source of such discrepancies lies in the fixing of the origins for X_s and R_s described in Sec. II, particularly as the origin of X_s was based on the μ SR value of λ_0 for optimally doped Tl2201, not measured on our own sample, and it has not proved possible to check this value. To put this in perspective, however, our estimated errors in fixing these origins are about $\pm 10^{-3}\Omega$ in X_s and about $\pm 10^{-4}\Omega$ in R_s , whereas, as inspection of Fig. 1(a) shows, the adjustments needed to give the expected normal state behavior are of order $10^{-1}\Omega$, larger than X_s itself in the superconducting state, and nearly 100 times larger than R_s . Adjustments of this size would lead to nonsensical conclusions in the superconducting state. For instance, subtracting fixed quantities from X_s so as to make X_s equal to R_s in the normal state would make X_s and λ_0 *negative* in the superconducting state and adding fixed quantities to R_s at 14 and 25 GHz so as to make R_s proportional to $\omega^{1/2}$ in the normal state would imply very large low temperature losses at these

frequencies in the superconducting state which could not be reconciled with the very narrow bandwidths observed. We conclude that errors in fixing the origins of R_s and X_s cannot possibly explain the discrepancies which we have observed in the normal state in Tl2201.

Because changes in X_s are observed as shifts of resonant frequency, differential errors in X_s may be produced by thermal expansion. The cavity itself is held at fixed temperature and does not expand, but there are small effects due to the movement of the sample as the sapphire rod expands and the expansion of the sample itself. The effect of expansion of the sapphire rod was deduced from frequency measurements made during the calibration using the replica Nb sample, and allowed for. The further error due to the difference between the expansions of the sample and the Nb replica was computed and shown to be equivalent at T_c to a change in λ of less than $0.05\lambda_0$, corresponding to a correction to X_s in the normal state of less than 1%. Moreover, this correction has a form as a function of temperature and frequency different from that of the observed discrepancy in X_s .

Errors in shaping the replica would lead to a scaling error in the resonator constant, but this could not explain our observations. We can also show that no combination of errors in the resonator constant, thermal expansion correction and the value assumed for λ_0 could account for what was observed.

Because the significant comparison is always between the observation with sample present and the corresponding observation with the calibrating replica present, the cavity perturbations are always very small. We expect the second order effects due to changes in the response of the remainder of the cavity induced by changes in the sample to be about 1 part in 10^4 smaller than the first order effects of the sample.

Strictly speaking, since our sample does not have cylindrical symmetry, some current flows in the c direction, and surface roughness can have the same effect. However, model calculations showed that these were small effects, and this was confirmed by the observation (in Bi2212 samples) that our results were independent of sample aspect ratio (which alters the proportion of current flowing in the c direction). The form of fit to the two-fluid model below T_c also suggests that there is no important c -axis contribution.

In Tl2201 the microwave skin depth δ is about $\frac{1}{4}$ of the sample thickness in the normal state at the lowest frequency. Model computation in one dimension, as performed for the Bi2212 samples, suggests that the thin sample corrections to the bulk surface impedance should be only 1–2%; they would also be in the opposite sense to what we observed: the thin sample effect should make X_s *smaller* than R_s , and should make R_s *less* frequency dependent at low frequencies. Nevertheless, δ may not be small compared to the rounding of the sharp edges of the sample, and since the current density is high there, this might have an important effect not covered by our model calculation. It is therefore important to note that this effect, too, cannot explain our observations, for by combining frequency and temperature values appropriately, we can choose observations at different frequencies at which the skin depth should be the same (on the standard model). In such a case any effect of the sharp edges should be the same for both, and the surface impedance, which is equal to $i\omega\mu_0\delta$, should simply scale as frequency. Inspec-

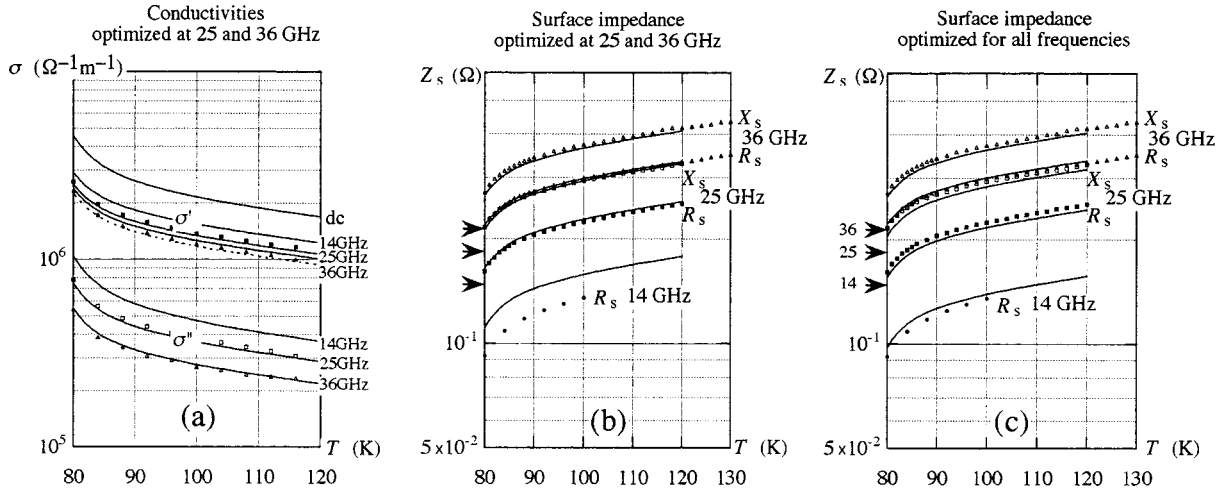


FIG. 5. Fits using an extra pole in the conductivity (solid lines), compared with data for TI2201. (a) Conductivities for fit optimized at 25 and 36 GHz; the dotted line shows σ_0 . (b) Corresponding surface impedance. (c) Surface impedance fit optimized at all three frequencies. The arrows show how the values of $R_s = X_s$ would have been spaced for the usual model of a real frequency-independent conductivity.

tion shows that this is far from true for our data.

In summary, we cannot find any experimental error large enough to explain the observed effects. Moreover, it is instructive to compare closely the behaviors of the TI2201 and Y123/Zn samples shown in Fig. 1. As we noted in Sec. II, for the Y123/Zn sample we have adjusted the origin of X_s to make $X_s = R_s$ in the normal state. This is a less satisfactory procedure than using an independent measurement of λ_0 , because it involves an assumption and is usually considerably less accurate. In this case, however, we have the reassurance of seeing that it has led to values of λ_0 which are plausible and only slightly different at 25 and 36 GHz. As we noted above, if we had adopted the same procedure for the TI2201 sample, we should have obtained nonsensical *negative* values for λ_0 . In both TI2201 and Y123/Zn the surface impedance data as plotted behave understandably below 70 K. In particular between 40 and 70 K in both materials R_s is quite closely proportional to ω^2 , the usual result for a superconductor when $\omega\tau$ is small. It is striking that in the normal state at 85 K, only 15 K higher, the behaviors are so different. For the Y123/Zn sample the frequency dependence of R_s accords exactly with the usual theory, whereas for the TI2201 sample the frequency dependence of R_s differs markedly from the usual theory and X_s differs from R_s by a wide margin. It is particularly difficult to envisage an experimental error which could have set in so suddenly over a 15 K range of temperature as to produce the effects observed in the normal state in TI2201, without any corresponding effect being visible at lower temperatures, or for the Y123/Zn sample (or, indeed, for our various Bi2212 samples). For these reasons we are inclined to take seriously our unusual normal state results in TI2201, even though we have not so far been in a position to check them on a second sample.

V. THE EXTRA NORMAL STATE CONDUCTIVITY IN TI2201

It is sometimes helpful to describe the conductivity in terms of its poles as a function of frequency. The conductivity observed in the normal state of TI2201 differs from that expected according to Eq. (3) chiefly in having an extra

imaginary component which is roughly proportional to $1/\omega$, while its real part falls slightly with increasing frequency (Fig. 2). This suggests the presence of an extra pole near $\omega = 0$. We have therefore explored the possibility of extending Eq. (3) by writing

$$\sigma = \sigma_0 + \frac{\sigma_+}{1 + i\omega\tau}, \quad (4)$$

where σ_0 is a frequency-independent conductivity [perhaps the conductivity expected according to Eq. (3), on the assumption that $\omega\tau_{GL}$ is small], and, in the new second term, $\omega\tau$ is quite large at the microwave frequencies of interest. (We examine the physical significance of such a term in the next section.)

This model does not match the data exactly, and we have some flexibility in selecting the best fit. For instance, Figs. 5(a) and 5(b) show a fit optimized for our observations at 25 and 36 GHz; the observed surface impedances are fitted within about 2%, but there is a 20% disagreement in the surface resistance at 14 GHz. Figure 5(c) shows an alternative fit optimized at all three frequencies; it agrees with all the surface impedance data within about 5%. However, this fit corresponds to a dc conductivity considerably greater than that measured in samples of similar doping. (We have not been able to make a reliable measurement of σ_{dc} in our microwave sample.) One can improve the fit to the expected value of σ_{dc} by moving the pole away from the imaginary axis, but this would imply a resonant response and it seems unreasonable to introduce such a model without stronger evidence or motivation. Though not perfect, Eq. (4) clearly works much better than the assumption that the conductivity is real and independent of frequency which is in error by as much as 60% in the surface impedance (arrows in Fig. 5).

The parameters of the extra term fitted are shown as functions of T in Fig. 6, for the fit optimized at 25 and 36 GHz. The term might be interpreted, for instance, as the response of some small group of electrons, whose density rises as we approach T_c (and is of the same order of magnitude as the predicted fluctuating density of superelectrons), but with a relaxation time τ which varies only weakly with T and is

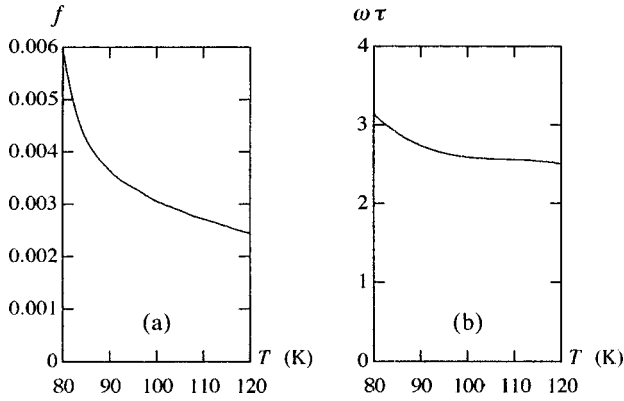


FIG. 6. Parameters of the proposed extra term, optimized at 25 and 36 GHz. (a) Fraction of electronic weight. (b) Value of $\omega\tau$ at 36 GHz.

much greater than the Ginzburg-Landau relaxation time τ_{GL} . On such an interpretation, the fit to the electronic weight is fairly robust, but the value of $\omega\tau$ is about doubled for the alternative fit mentioned above, though it remains fairly independent of T .

VI. POSSIBLE EXPLANATIONS OF THE EXTRA NORMAL STATE CONDUCTIVITY IN TI2201

We now adopt Eq. (4) as a rough description of what we have observed in TI2201, and make very tentative suggestions as to how such an expression might arise. A conceivable reason for the appearance of a new pole in the conductivity is that we have present an extra carrier of unconventional type, such as uncondensed bipolarons.¹⁰ On such a model, the electronic fraction shown in Fig. 6 must be interpreted as $(n_{bp}/n_e)(m_e/m_{bp})$, corresponding to a bipolaron density which rises as we approach T_c ; and since the bipolaron mass m_{bp} is probably much greater than the electron mass, would imply a substantial concentration of bipolarons. A scattering time τ with weak T dependence might also suit such a model. An obvious difficulty is that the effect has been seen only in TI2201. It has, however, been argued that the bipolaron density should be higher in underdoped samples. It is therefore important to repeat our experiment in samples with a range of dopings.

Less dramatic explanations must be explored also. Consider, for instance, the following interpretation of the theory of Aslamazov and Larkin. In their theory the fluctuation supercurrent decays with relaxation time τ_{GL} . Their theory does not involve flux lines explicitly, but if it remains true in the fluctuating region above T_c that supercurrent involves a phase gradient in the order parameter, then a supercurrent can only relax if flux lines pass through the system. Presumably we should treat the fluctuations in a single CuO_2 plane above T_c as generating some equilibrium density n_Φ of flux pancakes (two-dimensional flux lines) pointing in the c direction, with the same density of antflux pancakes pointing in the opposite direction, and we might guess that $n_\Phi \approx 1/2\xi^2$. Various forces act on these pancakes. In particular, if the system carries a supercurrent density J_s in the a direction, there will be forces $\pm J_s \Phi_0 t$ acting in the b direction on the flux pancakes and antflux pancakes. We may expect

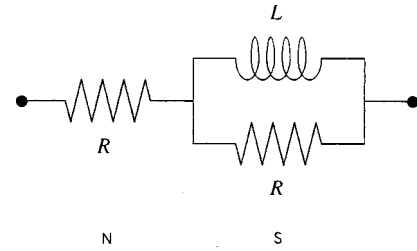


FIG. 7. Equivalent circuit for the series model.

such singularities to have a diffusion coefficient D of order ξ^2/τ_{GL} and to drift under the influence of an applied force f at velocity $v = Df/kT$. But the flow of flux-pancakes is associated with an electric field $E = n_\Phi \Phi_0 v$ (and the flow of antflux pancakes gives a second contribution to E having the same sign and magnitude). We deduce that $E \approx (2n_\Phi \Phi_0)(D/kT)(J_s \Phi_0 t) \approx [(4h(T - T_c)/e^2 T) J_s]$. This corresponds to a supercurrent fluctuation conductivity of the form Eq. (2) predicted by Aslamazov and Larkin.

From this point of view we might be able to explain Eq. (4) by recalling that there are other forces which might act on moving flux pancakes, not included in the theory of Aslamazov and Larkin. For instance, weak pinning forces due to inhomogeneities in the interaction energy might decrease the diffusion constant for flux pancakes, leading to a longer relaxation time for the supercurrent. This would lead to a term of the type suggested by Eq. (4) having at least approximately the weight observed. In such a model we would expect τ and hence σ_{dc} to be sample dependent, which could explain why the effect is not the same in all microwave samples. However, such an appeal to sample dependence is at odds with the general success of Aslamazov-Larkin theory in explaining observations of $\sigma_{dc}(T)$.

We have so far assumed that we simply add together a normal contribution to the conductivity, with a very short relaxation time, and a superconducting contribution with a longer one. This is correct when the two contributions flow independently and in parallel, as in the Aslamazov and Larkin theory. But we must remember that when we combine conductors in *series* the poles of the conductance may be moved. This suggests the following argument. Because of small variations in the local condensation energy, it may be that the pancakes and antipancakes are funnelled through particular regions in the sample. Above about 100 K we could ignore the fluctuation supercurrent in these regions, and treat them as normal (N). By contrast, the remainder of the material (S), if no flux lines flow through it, will carry undamped fluctuation supercurrent in parallel with normal current. The situation corresponds to the equivalent circuit shown in Fig 7. For a unit cube, and for simplicity assuming that the current flows in series through equal volumes of N and S , we identify R as $1/2\sigma_n$ and $i\omega L$ as $1/(-2i\sigma'')$, where σ_n is the normal conductivity (taken to be the same in both regions) and $-i\sigma''$ is the undamped supercurrent conductivity in S , which is proportional to $1/\omega$. We then easily find that the effective conductivity is

$$\sigma = \sigma_n + \frac{\sigma_n}{1 + i\omega\tau}, \quad (5)$$

where $\omega\tau=2\sigma_n/\sigma''$. This has precisely the form of Eq. (4), and the parameters have the required order of magnitude.

The difficulty with this simple model is that it assumes that there is easy conversion of supercurrent to normal current at the boundaries between the N and S regions, whereas we shall argue in Sec. VIII that according to the usual theory there should be little conversion outside the critical region. In the absence of conversion the Aslamazov and Larkin result would be little affected: the overall relaxation of the supercurrent would simply be determined by the flow of pancakes in the N regions, and would be too rapid to explain our observations. On the other hand, if the fluctuating gap parameter is higher in S than in N , we might expect a small amount of Andreev reflection of low-lying excitations as they approach S , with conversion of normal current to supercurrent. We do not attempt here to discuss whether this effect is large enough to explain our observations, but this question should be investigated.

VII. EFFECTIVE MEDIUM THEORY IN THE CRITICAL REGION

Within about 2 K of T_c , there is a sharp peak in σ' which rises with decreasing frequency, while σ'' falls from a value much greater than σ_{dc} just below T_c to a value much smaller than σ_{dc} just above T_c (Fig. 10). This is the region where we expect to observe critical fluctuations. When these fluctuations are large we expect that relatively large quasistatic regions (of order ξ_{GL} in scale) will be either normal (N) or superconducting (S), the sizes of these regions remaining, however, normally much smaller than the grains or the microwave skin depth. As we shall argue in Sec. VIII, it seems reasonable to suppose that within the critical region normal current is converted to supercurrent at the NS boundaries, without substantial boundary resistance. We are not aware of any precise discussion of this situation which could be used to predict the effective conductivity at microwave frequencies. In these circumstances it seemed to us reasonable and instructive to make use of effective medium theory, which is designed to predict the conductivity of a mixture of two materials, with conductivities σ_n and σ_s which will in general be complex at microwave frequencies.

Precise effective medium theory would require a knowledge of the shapes and arrangements of the N and S regions, which we do not have. We have therefore used the theory of general type employed by Cohen and Jortner,¹¹ based on earlier work by Landauer and others.¹² According to this theory the effective measured conductivity $\sigma=\sigma'-i\sigma''$ is given, in a three-dimensional system, by the root of the quadratic equation

$$2\sigma^2 - [(3C-1)\sigma_s + (3\tilde{C}-1)\sigma_n]\sigma - \sigma_n\sigma_s = 0, \quad (6)$$

where C is the proportion of S material and $\tilde{C}=1-C$ is the proportion of N material. The reasoning behind this equation is explained in the original papers; its derivation remains valid when the conductivities are complex. At zero frequency $\sigma_s \rightarrow \infty$, and approaching T_c from above we find the solution

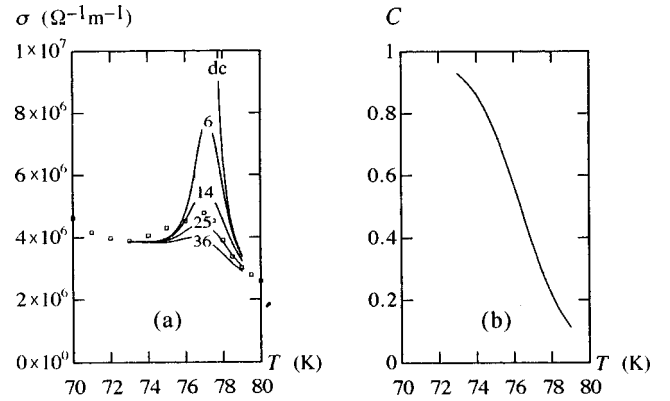


FIG. 8. (a) Effective medium predictions of σ' at several frequencies based on a simple model; the data points shown are for TI2201 at 25 GHz. (b) Form of $C(T)$ used.

$$\sigma_{dc} = \frac{\sigma_n}{1-3C} \quad (7)$$

which diverges as C approaches $\frac{1}{3}$. This point represents the *percolation limit* at which the superconducting regions first join up to provide a dc zero-resistance path across the whole sample, which we identify as the critical temperature T_c .

At microwave frequencies σ_s is no longer infinite, but has a large imaginary component, proportional to $1/\omega$, which for the lower microwave frequencies is much greater than σ_n . The effective conductivity predicted by Eq. (6) no longer diverges at T_c , but its real part σ' shows a sharp peak there. At T_c we find that

$$\sigma \approx \sqrt{\frac{\sigma_n\sigma_s}{2}} \quad (8)$$

with approximately equal real and imaginary parts proportional to $\omega^{-1/2}$. As may be seen from Figs. 2 and 10, this accords with our observations. To illustrate the behavior of Eq. (6) we show in Fig. 8 the peaks in $\sigma'(T)$ which arise for a simple two-fluid model in which we take $\sigma_s = \sigma'_s - i\sigma''_s$ and $\sigma_n = \sigma'_n$, with σ'_s and σ'_n independent of frequency and σ''_s proportional to $1/\omega$. For simplicity we have treated σ_s and σ_n as independent of temperature also and adjusted their values to fit our 25 GHz data in TI2201 for σ at 73 K and for σ' at 79 K, temperatures just below and just above the critical region. As shown in the figure, $C(T)$ was chosen as a suitable symmetrical function (in fact a Fermi function of characteristic width 1.3 K centered at 76.4 K). The corresponding predictions for $\sigma''(T)$ fall from a value below T_c much greater than σ'_n to a negligible value above T_c . These theoretical conclusions are understandable when we recall that just above T_c the current is flowing in *series* through S and N regions, with the S regions almost touching, whereas below T_c we have a continuous superconducting network of high conductivity in *parallel* with effectively normal regions of lower conductivity, consisting of a normal matrix containing isolated and almost touching superconducting regions. It is clear that an effective medium model of this type is capable of giving a good qualitative account of the behavior observed in $\sigma'(T)$.

To take the argument further, we need more carefully considered values for $\sigma_s(T)$, $\sigma_n(T)$, and $C(T)$. For the the-

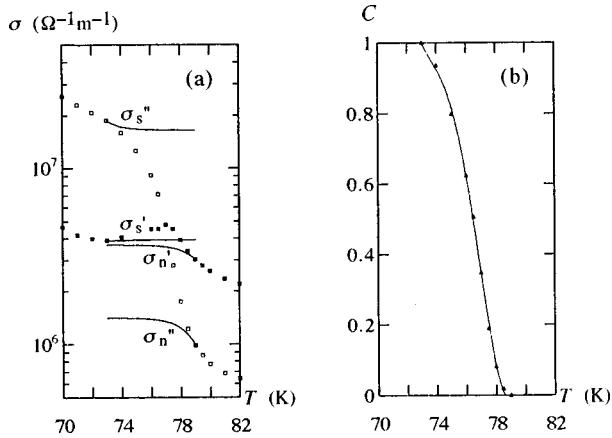


FIG. 9. (a) The values of $\sigma_s(T)$ and $\sigma_n(T)$ used in fitting for TI2201 at 25 GHz (solid lines), compared with observed conductivities. (b) Deduced values of $C(T)$, with fitted smooth curve.

oretical curves fitted to the data on TI2201 shown in Fig. 10 we proceeded as follows. We first chose temperatures below and above T_c at which we judged that critical effects were just becoming apparent. Below T_c we chose 73 K as the temperature at which downward curvature begins in $\sigma''(T)$ (Fig. 10). Above T_c we chose 78 K as the temperature at which the Ginzburg plot of $1/\sigma_{\text{fluc}}$ against T departs from linearity (Fig. 3); this temperature was later revised upwards slightly, as described below. We argued that at the lower temperature the value and temperature derivative of $\sigma_s(T)$ should match those of the observed $\sigma(T)$, and that at the upper temperature those of $\sigma_n(T)$ should match the observed $\sigma(T)$, for each frequency. However, we know that the fluctuations become large within the critical region, and our argument is based on the idea that the N and S regions have substantially different properties there. We therefore assumed that σ_s and σ_n become independent of T as we enter the critical region. In fact we chose to make these quantities become flat exponentially, with a characteristic exponential range of 1 K, as shown in Fig. 9 for the 25 GHz data. (The quality of fit was not sensitive to the precise value chosen for this range, and we did not vary it in fitting the data. Our choice implies that Δ is not less than $0.7kT$ in the S regions.) Having chosen $\sigma_s(T)$ and $\sigma_n(T)$, and knowing $\sigma(T)$, we solved Eq. (6) for $C(T)$, which should of course be real. Using the 25 GHz data we found that it was possible to make the imaginary part of C small over the whole of the temperature range by increasing the upper temperature boundary

from 78 to 79 K; the resulting values of $C(T)$ are shown in Fig. 9, with a smooth curve fitted to them. Finally, having chosen $\sigma_s(T)$ and $\sigma_n(T)$ for all frequencies and obtained a smooth form for $C(T)$ from the 25 GHz data, we solved Eq. (6) for σ at all three frequencies; the resulting predictions are shown in Fig. 10.

[At 14 GHz, where we had no surface reactance data, the conductivity data points above 73 K shown in Fig. 10 were obtained as follows. Above 79 K the complex conductivity was obtained using the model described in Sec. V, with a small adjustment of $\omega\tau$ so that $R_s(T)$ at 14 GHz was fitted exactly rather than approximately. Values of σ'' between 73 and 79 K were then predicted using effective medium theory, as described above. Finally these values were used in computing the σ' data points between 73 and 79 K from the observed values of $R_s(T)$.]

It might be argued that the critical fluctuations in the CuO_2 planes should be two-dimensional. In such a case Eq. (6) is replaced by

$$\sigma^2 - [(2C - 1)\sigma_s + (2\tilde{C} - 1)\sigma_n]\sigma - \sigma_n\sigma_s = 0 \quad (9)$$

and the percolation limit corresponding to T_c occurs when $C = \frac{1}{2}$; at this point we now have $\sigma = \sqrt{\sigma_n\sigma_s}$ exactly. We have refitted our data using this equation, and found that the fit is almost equally good. [In this case we found the best fit when we chose the upper boundary of the critical region to be 79.5 K, and the required form for $C(T)$ is moved slightly higher in temperature. Apart from a small increase in the predicted peak heights, the conductivity fits were very similar to those shown in Fig. 10.]

Effective medium theory describes the transport currents which flow through the medium in response to an electric field. We ought also, in principle, to take account of screening currents which circulate inside the superconducting regions in response to a magnetic field. Such currents alter the effective magnetic permeability of the medium, and this should be included in the skin depth analysis. However, because the coherence length is so much smaller than the penetration depth in the cuprates this effect is negligible in the critical region (and even smaller in the region of small fluctuations considered in Sec. III); we have ignored it in our analysis.

Considering the crudeness of this model we are encouraged by the quality of the fit shown in Fig. 10. We varied only one parameter (the upper temperature) in fitting the

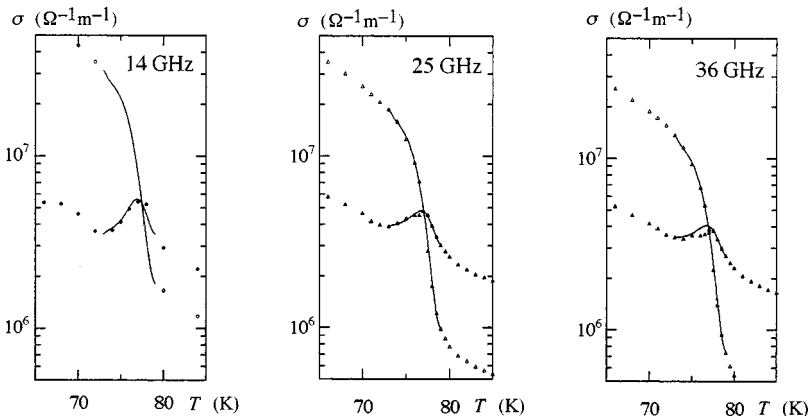


FIG. 10. Conductivities of TI2201 in the a - b plane near T_c at three frequencies. The solid lines are the fits to effective medium theory within the critical region.

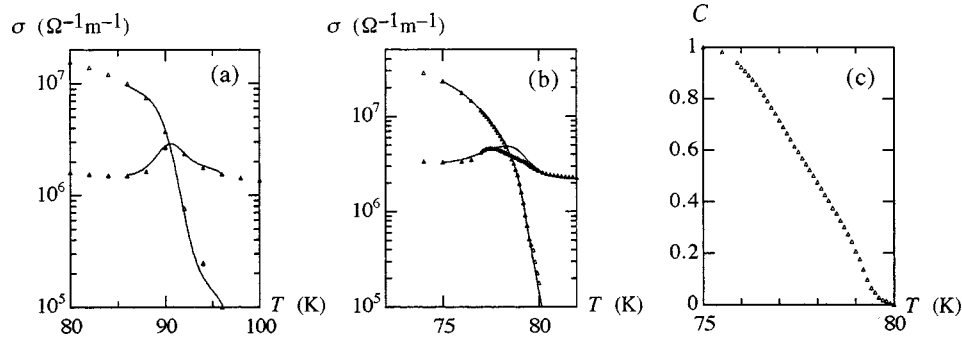


FIG. 11. Two-dimensional effective medium fits for other samples. (a) Bi2212 at 35 GHz. (b) Y123/Zn at 25 GHz. (c) $C(T)$ for (b).

data. Moreover, the agreement with the striking observation that $\sigma' \approx \sigma''$ at the peaks was independent of this parameter, and the agreement with the observed peak heights was only weakly dependent on it. We also note that the single form for $C(T)$ (i) gives a good fit for $\sigma''(T)$ at both 25 and 36 GHz (in a region in which σ'' falls by a factor of about 30), (ii) provides a good fit to the peaks in $\sigma'(T)$ at 14 GHz and 25 GHz, and a reasonable fit at 36 GHz, and (iii) is approximately symmetrical, its width agreeing with other measures of the width of the critical region.

We obtained fits of equally good quality using the same method for our Bi2212 data in the critical region: an example of a two-dimensional fit is shown in Fig. 11(a). However, for Y123/Zn [Figs. 11(b), 11(c)] the observed peak in σ' was asymmetric, and no longer occurred at the point where $\sigma' = \sigma''$. We could not find sensible forms for $C(T)$, $\sigma_s(T)$, and $\sigma_n(T)$ which fitted the data, and the usual procedure, though it fitted $\sigma''(T)$ well, generated a form for $C(T)$ broader and less symmetric than those for the Tl2201 and Bi2212 samples, and a peak in $\sigma'(T)$ at the wrong T . We believe that the reason for these observations lies in the fact that the critical temperature of Zn-doped Y123 is sensitive to the level of doping and will therefore be slightly inhomogeneous if the sample is not perfectly annealed. Inhomogeneities on a *fine* scale would simply increase somewhat the local inhomogeneities produced by the critical fluctuations, leading to results essentially similar to those seen in the other materials. But inhomogeneities on a scale larger than the skin depth would mean that the observed surface impedance is averaged over a range of T_c values. At most temperatures this will be about the same as the true surface impedance for the mean value of T_c , but in the immediate neighborhood of T_c both R_s and X_s will be depressed below this value, because their slopes change suddenly at this point, with R_s depressed more because it falls more sharply. This turns out to have the effect, when we compute σ from Z_s , of increasing the apparent value σ'' while leaving σ' almost unchanged. This in turn moves $\sigma''(T)$, $C(T)$, and the predicted $\sigma'(T)$ to higher T values, providing a natural explanation of the discrepancies observed.

It is worth noting that we have also been able to fit our earlier data obtained by the powder method^{4,13} at frequencies of about 6 GHz, where the peak is much higher, by similar methods. In optimized Y123 the temperature spread of $C(T)$ was similar to that reported here, but in Y123 doped with various levels of Zn and Co we found that it was often considerably greater, suggesting that doping inhomogeneities

have generated a spread of T_c values. We conclude, in the absence of a more exact theory, that there is no reason to ascribe the effects observed near T_c in optimized samples of Tl2201, Bi2212, and probably Y123 to anything other than critical fluctuations.

VIII. CONVERSION OF NORMAL CURRENT TO SUPERCURRENT WITHIN FLUCTUATING REGIONS

We now discuss our assumptions about the conversion of normal current to supercurrent at boundaries between a normal region (N) and a superconducting region (S) when there are fluctuations present.

The theory of NS interfaces¹⁴ is usually applied to situations such as an NS junction between two metals or at the NS interfaces between domains of the intermediate state of type I superconductors. According to this theory, normal electron current arriving at an interface delivers an excess of electronlike excitations to the interface, and this excess decays by two processes occurring near the interface: *Andreev processes* in which electrons are reflected as holes, and *branch-crossing scattering processes* in which electrons are scattered as holes or pairs of electrons are annihilated. Each of these processes injects a condensed pair of electrons into the superconductor.

For fluctuations in Tl2201 above the critical region we remarked in Sec. III that Δ , the gap parameter inside the fluctuating S regions, is typically $0.2kT$. In such a situation at a conventional NS interface most arriving electrons would not be Andreev reflected and would enter the S region. An electron excess would extend a distance $\lambda_Q = \sqrt{l_0 l_Q/3}$, the *diffusion length for branch crossing*, into the S region, where l_0 and l_Q are, respectively, the mean free paths for all scattering and for branch-crossing processes, and in this region the electrochemical potentials μ_n and μ_s for normal and superelectrons would differ. The electron excess would be associated with an excess boundary resistance. However, in the cuprates the size ξ_{GL} of the fluctuating S regions is much less than λ_Q . In this situation the electron excess created on one side of the S region should cancel the electron deficit created on the opposite side, and the charge excess, the excess boundary resistance, and the conversion of normal to supercurrent should all become negligible. This is what is assumed by the Aslamazov and Larkin theory, which treats the normal and superconducting transport processes as independent. However, as we noted in Sec. VI, some small degree of conversion may still be present above T_c .

Within the critical region, on the other hand, the N and S regions become much larger, and, as we noted in Sec. VII, the gap parameter Δ inside the fluctuating S regions is typically $0.7kT$. We would now expect Andreev reflection to be the dominant conversion process. At a conventional NS interface the wave functions of the Andreev reflected electrons would have exponential tails extending a distance ξ_{GL} into the S region. For cuprates within the critical region ξ_{GL} must be calculated for the value of Δ inside the S regions, and is relatively short, whereas the size of the S regions diverges at T_c . Thus we expect that transmission by tunneling through the S regions should become negligible, Andreev reflection should be effective, normal current will be converted to supercurrent, and the boundary resistance should be small. This is what we assumed in Sec. VII.

IX. DISCUSSION AND CONCLUSIONS

Our conductivity data above T_c for Bi2212 appeared to agree quite well in form and magnitude with two-dimensional Aslamazov and Larkin theory, adapted to high frequency (Sec. III). This is not surprising, for the interplane coupling is known to be weak in this material. Y123/Zn also fitted the two-dimensional theory quite well in form, but with a considerable discrepancy in scaling, the effective value of t being about $2c$. The parent compound Y123 has relatively strong interlayer coupling, and measurements of heat capacity and dc conductivity⁹ show a transition from three-dimensional to two-dimensional fluctuations between 100 and 110 K. Our results may be naturally explained on the assumption that Zn doping weakens the interlayer coupling, but not by enough to reach the two-dimensional limit. We

should perhaps also recall that the Aslamazov and Larkin theory was worked out for s -wave superconductors. The general arguments given in Sec. III suggest that the theory will retain the same form if the cuprates are in fact d -wave materials, as is now widely believed, but we might expect significant scaling factors.

The anomalous extra conductivity found in Tl2201 above the critical region may prove to be important but remains mysterious at present. None of the three possible explanations discussed in Sec. VI seems very satisfactory, and for none of them is it clear why the effect has appeared in Tl2201 and not in the very similar material Bi2212. The next step must be to find how reproducible the effect is, and how it is related to electron doping, flux pinning, and the dimensionality of fluctuations.

The discussion of conductivity within the critical region in terms of effective medium theory (Sec. VII) is broadly satisfactory, and suggests strongly that the well-known peak in $\sigma'(T)$ is simply a critical phenomenon. It would, however, be helpful to have some theoretical confirmation that the method adopted for choosing $\sigma_s(T)$ and $\sigma_n(T)$ within the region of critical fluctuations is reasonable.

ACKNOWLEDGMENTS

We are particularly grateful for supply of high quality crystals by T. Mochiku (Bi2212), A.P. Mackenzie and A.L. Tyler (Tl2201), and J. Hodby (Y123/Zn). We also acknowledge helpful discussions with them, and with J. Cooper, J. Loram, W.L. Hardy, and D. C. Bonn. The work was funded by EPSRC, with additional support from the Government of Australia.

¹Shih-Fu Lee, D. C. Morgan, R. J. Ormeno, D. M. Broun, R. A. Doyle, and J. R. Waldram, Phys. Rev. Lett. **77**, 735 (1996); D. M. Broun, D. C. Morgan, R. J. Ormeno, S. F. Lee, A. W. Tyler, A. P. Mackenzie, and J. R. Waldram, Phys. Rev. B **56**, R11 443 (1997); J. R. Waldram *et al.* (unpublished).

²D. A. Bonn, Ruixing Liang, T. M. Riseman, D. J. Baar, D. C. Morgan, Kuan Zhang, P. Dosanjh, T. L. Duty, A. MacFarlane, G. D. Morris, J. H. Brewer, W. N. Hardy, C. Kallin, and A. J. Berlinsky, Phys. Rev. B **47**, 11 314 (1993); A. John Berlinsky, C. Kallin, G. Rose, and A.-C. Shi, *ibid.* **48**, 4074 (1993); P. J. Hirschfeld, W. O. Putikka, and D. J. Scalapino, *ibid.* **50**, 10 250 (1994); J. R. Waldram, P. Theopistou, A. Porch, and H.-M. Cheah, *ibid.* **55**, 3222 (1997).

³M. Tinkham, *Introduction to Superconductivity*, 2nd ed. (McGraw-Hill, New York, 1995), p. 287; L. Tewordt, D. Fay, and T. Wolkhausen, Physica C **153-155**, 703 (1988); Ref. 8.

⁴A. Porch, J. R. Waldram, and Lesley Cohen, J. Phys. F **18**, 1547 (1988); K. Holczer, L. Forro, L. Mihály, and G. Grüner, Phys. Rev. Lett. **67**, 152 (1991); John R. Waldram, Adrian Porch, Horn-Mun Cheah, and Shih-Fu Lee, Physica B **194-196**, 1607 (1994); D. A. Bonn, D. C. Morgan, Kuan Zhang, Ruixing Liang, D. J. Barr, and W. N. Hardy, J. Phys. Chem. Solids **54**, 1297 (1993).

⁵T. Mochiku and K. Kadowaki, Trans. Mater. Res. Soc. Jpn. **19A**,

349 (1993).

⁶R. J. Ormeno, D. C. Morgan, D. M. Broun, S. F. Lee, and J. R. Waldram, Rev. Sci. Instrum. **68**, 2121 (1997); D. M. Broun *et al.* (unpublished).

⁷Y. J. Uemura, A. Keren, L. P. Lee, G. M. Luke, W. D. Wu, Y. Kubo, T. Manako, Y. Shimakawa, M. Subramanian, J. L. Cobb, and J. T. Markert, Nature (London) **364**, 605 (1993).

⁸L. G. Aslamazov and A. I. Larkin, Fiz. Tverd. Tela (Leningrad) **10**, 1104 (1968) [Sov. Phys. Solid State **10**, 875 (1968)].

⁹J. W. Loram, J. R. Cooper, J. M. Wheatley, K. A. Mirza, and R. S. Liu, Philos. Mag. B **65**, 1405 (1992).

¹⁰A. S. Alexandrov and J. Ranninger, Phys. Rev. B **23**, 1796 (1981); **24**, 1164 (1981); A. S. Alexandrov and N. F. Mott, Phys. Rev. Lett. **71**, 1075 (1993).

¹¹M. H. Cohen and J. Jortner, Phys. Rev. Lett. **30**, 696 (1973).

¹²R. Landauer, J. Appl. Phys. **23**, 779 (1952); S. Kirkpatrick, Phys. Rev. Lett. **27**, 1722 (1971).

¹³J. R. Waldram, A. Porch, and H.-M. Cheah, Physica C **232**, 189 (1994); A. Porch, H.-M. Cheah, and J. R. Waldram, Physica B **165-166**, 1197 (1990).

¹⁴A. B. Pippard, J. G. Shepherd, and D. A. Tindall, Proc. R. Soc. London, Ser. A **324**, 17 (1971); T. Y. Hsiang and J. Clarke, Phys. Rev. B **21**, 945 (1980); J. R. Waldram and S. J. Battersby, J. Low Temp. Phys. **86**, 1 (1992).